



Image reconstruction from incomplete projection data by means of iterative algebraic algorithms

Nadiya Gubareni¹ and Mariusz Pleszczyński²

¹ Politechnika Częstochowska,
ul. Dąbrowskiego 69, 42-200 Częstochowa, Poland

gubareni@zim.pcz.pl,

² Politechnika Śląska,
ul. Kaszubska, 23, 44-101 Gliwice, Poland
dm101live@interia.pl

Abstract. In this paper we consider the problem of image reconstruction from incomplete projection data for some particular schemes of reconstruction. We present the numerical reconstruction algorithms for image reconstruction of high contrast objects from incomplete data. Numerical simulation results for a number of modeling objects with high contrast are presented and discussed.

1 Introduction

In the recent years technique of computerized tomography found a wide application not only in medicine but also for solving many technical problems. In all these applications we deal with inverse problems which are those of image reconstruction from projections. In spite of the wide different physical methods to collect projection data there is a common mathematical nature of reconstruction problems: there is an unknown distribution of some physical parameter. A finite number of line integrals of this parameter can be estimated from physical measurements, and an estimate of the distribution of the original parameter is desired.

In many applications the projection data are often not available at each angle of view and may be very limited in number. In particular, such kind of problems arises in mineral industries and engineering geophysics connected with acid drainage, the stability of mine workers, mineral exploration and others [9, 10].

For these problems the projection operator can be represented algebraically and the problem of image reconstruction is reduced to solving a system of linear algebraic equations. For solving such systems there often used different kinds of algebraic iterative algorithms the most well-known from which are ART and MART algorithms [1, 3–8]. They are generally simple, flexible and permit to use *a priori* knowledge of the object before its reconstruction that is very important in many practical applications.

In this paper we consider the problems of image reconstruction from incomplete projection data for some particular reconstruction schemes which arise in

some problems of engineering geophysics and mineral industry. For solving these problems we use the iterative algebraic algorithms. Numerical simulation of solving problems for image reconstruction from incomplete projection data for some modeling objects, comparing evaluations of errors and rate of convergence of these algorithms are presented. It is shown then for some choice of parameters we can obtain a good enough quality of reconstruction with these algorithms for some large number of iterations.

2 Problem of incomplete projection data

Let $f(x, y)$ be a function which represents the spatial distribution of a physical parameter. If L is a line (ray) in the plane then the line integral

$$p_L = \int_L f(x, y) dL, \quad (1)$$

which is usually called a projection, is usually obtained from physical measurements.

From mathematical point of view the problem of reconstruction from projections is to find an unknown function $f(x, y)$ by means of a given set of projections p_L for all L . This problem was solved by J. Radon in 1917 in the form of the inversion formula which expresses f in terms of p . Unfortunately, this mathematical problem represents only an idealized abstraction of problems which occur in practical applications. In practice we are given only discrete projection data that estimate p for a finite number of rays. And we want to find an image function $f(x, y)$, i.e. a reconstructed estimate of the unknown object. Moreover, we are deal with limited precision of measured data and so the projection data are given with some errors. Therefore all these restrictions do not allow us to use the Radon inversion formula directly.

There exist two fundamentally different approaches for solving the image reconstruction problem. In one approach the problem is formulated for continuous functions f and p and the inversion formula is derived in this continuous model. This method is called the transform method approach [2]. The second approach is connected with discretization of the function f at the outset. The object f and measurements p then become vectors in the finite dimensional Euclidean space. And for solving this model we use the methods of linear algebra and optimization theory. This approach is called the fully discretized model [2].

If the number of projection data can be obtained large enough and for any directions then in these applications (in medicine, for example) it is more preferred to use the transform method approach. But in many practical applications the projection data cannot be available for each direction and its number is very limited. In this case we say that we have a problem of image reconstruction with incomplete projection data. In particular, such kind of problems arise in mineral industries and engineering geophysics connected with acid drainage, the stability of mine workers, mineral exploration and others [9, 10].

In dependence on the obtaining system of projections there are many image reconstruction schemes, the main of them are parallel and beam schemes in the two-dimensional space. Both of them are represented in Fig.1 and Fig.2.

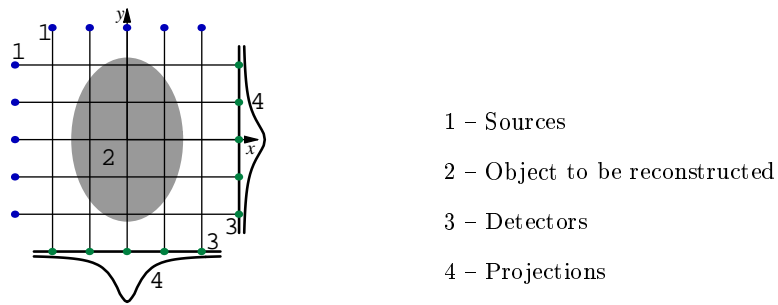


Fig. 1. Parallel scheme of image reconstruction

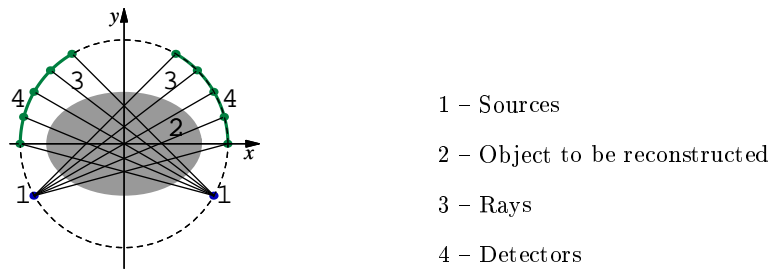
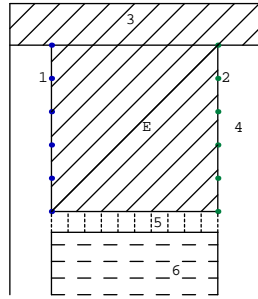


Fig. 2. Beam scheme of image reconstruction

In some practical problems, in engineering for example, it is impossible to get projections from all directions because of the existing some important reasons (such as situation, size or impossibility of an access to a research object). This situation arises, for example, in the coal bed working. In such a coal bed during the preparing process for working in dependence on the scheme the access to longwalls may be very difficult or impossible at all. Sometimes it is impossible to access to one or two sides of longwalls, and sometimes it is impossible only to access to the basis but all the longwalls are accessible. Each this situation has its own scheme of obtaining information.

In this paper we present results for image reconstructions only for two different schemes, which are described below.

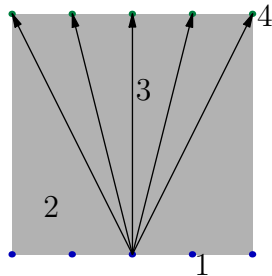


- 1 – Sources
- 2 – Detectors
- 3 – Unmined coal
- 4 – Heading
- 5 – Longwall with mechanized lining, belt conveyor flight, heading machine so on.
- 6 – Caving or filling
- E* – Researching coal bed

Fig. 3. The scheme of a coal bed working

2.1 System 1×1

Consider the scheme which is the worst from the view of obtaining projection data. In this scheme we have an access to a research coal bed from only two opposite sides. This situation often arise in engineering geophysics as well. In this case the sources of rays are situated only on one side and the detectors are situated on the opposite side of the research part of a coal bed. This scheme of obtaining information is shown in Fig.4 and we shall call it as the system 1×1 . As one may see this system is the most far from the common systems for image



- 1 – Sources of rays
- 2 – Research object
- 3 – Rays
- 4 – Detectors

Fig. 4. The system 1×1 .

reconstruction problems (see Fig.1 and Fig.2), where projections can be obtained from any direction.

2.2 System $(1 \times 1, 1 \times 1)$

Consider the situation when we can have an access to all four sides of a coal bed. In this scheme the sources are situated onto two neighboring sides, and the detectors are situated on the opposite sides. So the projections can be obtained from two pair of the opposite sides. This situation is shown in Fig.5 and we shall call it as the system $(1 \times 1, 1 \times 1)$.

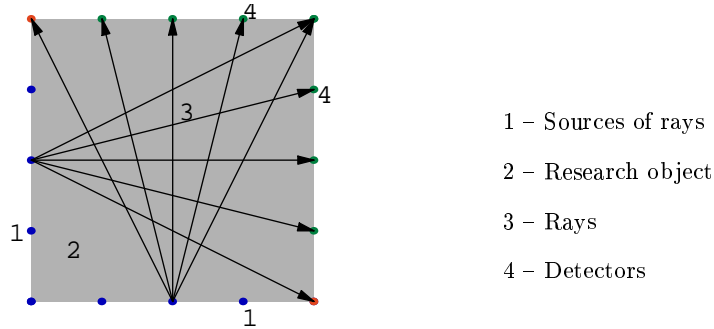


Fig. 5. The system $(1 \times 1, 1 \times 1)$

3 Reconstruction algebraic algorithms

At first, for constructing the full discrete model we include a reconstructed domain $D \subset R^2$ into a rectangle E and divide it into n small elements (pixels). The full discrete model of the problem of image reconstruction is based on the main principal that a research object has the constant distribution inside each pixel. So for any i -th pixel we can correspond an unknown x_i . Secondly, we assume that sources and detectors are points and the rays between them are lines. We denote by a_{ij} the length of the intersection of the i -th ray with j -th pixel. In this case the problem of image reconstruction is reduced to solving a system of linear algebraic equations:

$$\mathbf{A} \cdot \mathbf{x}^T = \mathbf{p}^T, \tag{2}$$

where:

- $\mathbf{A} \in R^{m,n}$ is the projection matrix,
- $\mathbf{x} \in R^n$ is the image vector,
- $\mathbf{p} \in R^m$ is the measurement vector of projection data.

This system has a few characteristics: it is a rectangular as a rule and it has a very large dimension. For solving this system it is often used different kind of algebraic iterative algorithms which are based on the Kaczmarz method, the most well-known of which are the additive algorithm ART and the multiplicative algorithm MART (see [1], [3]-[8]). These algorithms are very flexible and allow to apply different *a priori* information about object before its reconstruction that is especially very important when we have an incomplete projection data. The basic idea of these algorithms is to run through all equations cyclically with modification of the present estimate $\mathbf{x}^{(k)}$ in such a way that the present equation with index i is fulfilled.

In this paper we use some modifications of these algorithms which we call ART-3 and MART-3.

Algorithm ART-3

1. $\mathbf{x}^{(0)} \in R^n$ is an arbitrary vector.
2. The $k+1$ -th iteration is calculated in accordance with the following scheme:

$$\mathbf{x}^{(k+1)} = \mathbf{x}^{(k)} + S_k \frac{\mathbf{a}^{i(k)}}{\|\mathbf{a}^{i(k)}\|^2}, \tag{3}$$

where:

$$S_k = \begin{cases} 0, & \text{for } |p_i - (\mathbf{a}^{i(k)}, \mathbf{x}^{(k)})| \leq \varepsilon_i; \\ p_i - (\mathbf{a}^{i(k)}, \mathbf{x}^{(k)}), & \text{for } |p_i - (\mathbf{a}^{i(k)}, \mathbf{x}^{(k)})| \geq \varepsilon_i; \\ 2(p_i + \varepsilon_i - (\mathbf{a}^{i(k)}, \mathbf{x}^{(k)})), & \text{for } p_i + \varepsilon_i < (\mathbf{a}^{i(k)}, \mathbf{x}^{(k)}) < p_i + 2\varepsilon_i; \\ 2(-p_i + \varepsilon_i + (\mathbf{a}^{i(k)}, \mathbf{x}^{(k)})), & \text{for } p_i - 2\varepsilon_i < (\mathbf{a}^{i(k)}, \mathbf{x}^{(k)}) < p_i - \varepsilon_i, \end{cases} \tag{4}$$

where:

- \mathbf{a}^i is the i -th row of the matrix \mathbf{A} ,
 - p_i is the i -th coordinate of the projection vector \mathbf{p} ,
 - ε_i is a parameter which defines precision of a solution
- and $i(k) = k \pmod m + 1$.

This algorithm was investigated by G.T.Herman [6], and it was used successfully in medicine.

Algorithm MART-3

1. $\mathbf{x}^{(0)} \in R^n$ is an arbitrary vector and $\mathbf{x}^{(0)} > 0$.
2. The $k+1$ -th iteration is calculated in accordance with the following scheme:

$$x_j^{(k+1)} = \left(\frac{p_i}{(\mathbf{a}^{i(k)}, \mathbf{x}^{(k)})} \right)^{\lambda_k^i a_{ij}} x_j^{(k)}, \tag{5}$$

where:

- \mathbf{a}^i is the i -th row of the matrix \mathbf{A} ,
 - λ_k^i is a relaxation parameter,
 - p_i is the i -th coordinate of the projection vector \mathbf{p} ,
- and $i = k \pmod m + 1$.

This algorithm was invented and reinvented in several fields. It was shown that it is convergent if $0 < \lambda_k^i a_{ij} \leq 1$ for all i, k, j , and its solution gives the solution of the linearly constrained entropy optimization problem (see [2],[4],[8]).

In this paper we consider that $\lambda_k^i = \lambda = const$ for all i, j, k and we use algorithms ART-3 and MART-3 with following constraining operators:

$$C_1[\mathbf{x}] = \begin{cases} \mathbf{x}, & \text{if } \mathbf{x} \in D; \\ 0, & \text{otherwise} \end{cases} \quad (6)$$

$$(C_2[\mathbf{x}])_i = \begin{cases} a, & \text{if } x_i < a; \\ x_i, & \text{if } a \leq x_i \leq b; \\ b, & \text{if } x_i > b \end{cases} \quad (7)$$

$$(C_3[\mathbf{x}])_j = \begin{cases} 0, & \text{if } p_i = 0 \text{ and } a_{ij} \neq 0; \\ x_j, & \text{otherwise} \end{cases} \quad (8)$$

4 Computer simulation and experimental results

In order to evaluate the goodness of the compute reconstruction of a high-construct image from a limited number of projections and incomplete data we tested different kind of geometric figures and reconstruction schemes.

An important factor in the simulation process of image reconstruction is the choice of modeling objects which describe the density distribution of research objects. In a coal bed, where we search the reservoirs of compressed gas or interlayers of a barren rock, the density distribution may be considered discrete and the density difference of these three environments (coal, compressed gas and barren rock) is significant. Therefore for illustration of the implementation of the algorithms working with incomplete data we chose the discrete functions with high contrast. In this paper we present only the results of computer reconstruction for two discrete figures and two reconstructions schemes 1×1 and $(1 \times 1, 1 \times 1)$.

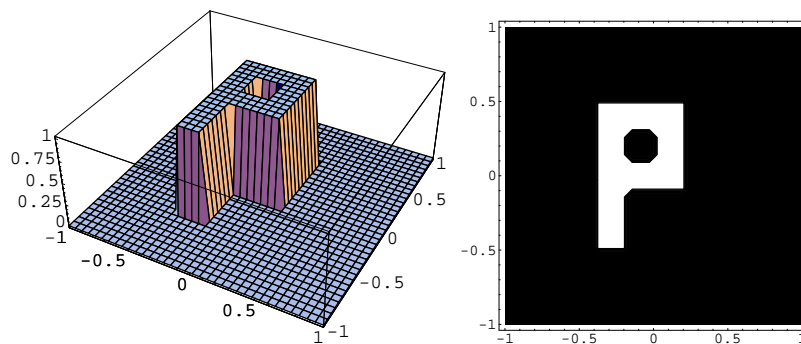


Fig. 6. The original function $f_1(x, y)$.

The first discrete function $f_1(x, y)$ is given by the following equation:

$$f_1(x, y) = \begin{cases} 1, & (x, y) \in D \subset E \subset \mathbb{R}^2, \\ 0, & \text{otherwise} \end{cases} \quad (9)$$

where E is a square $E = \{(x, y): -1 \leq x, y \leq 1\}$, and D is a subset of E of the following form:

$$D = [-0.4, -0.2] \times [-0.5, 0.5] \cup [-0.2, 0.2] \times [0.3, 0.5] \cup [-0.2, 0.2] \times [-0.1, 0.1] \cup [0, 0.2] \times [0.1, 0.3]. \quad (10)$$

The plot of this function is presented in Fig.6, where the figure on the left side is a three-dimensional view of the plot of $f_1(x, y)$, and on the right side it is represented the two-dimensional view of the plot of $f_1(x, y)$ (the black color denotes the value 0 and the white color denotes the value 1).

The second figure is given by the following equation:

$$f_2(x, y) = \begin{cases} 1, & (x, y) \in D_1 \subset E \subset \mathbb{R}^2, \\ 2, & (x, y) \in D_2 \subset E \subset \mathbb{R}^2, \\ 3, & (x, y) \in D_3 \subset E \subset \mathbb{R}^2, \\ 4, & (x, y) \in D_4 \subset E \subset \mathbb{R}^2, \\ 0, & \text{otherwise} \end{cases} \quad (11)$$

where E is a square $E = \{(x, y): -1 \leq x, y \leq 1\}$, and D_i are subsets of E of the following form: $D_1 = [-0.1, 0.3] \times [0.3, 0.4]$, $D_2 = [-0.3, -0.1] \times [-0.6, 0.6]$, $D_3 = [-0.4, -0.3] \times [0, 0.1]$, $D_4 = [-0.1, 0.2] \times [-0.4, -0.3]$. The plot of this function is given in Fig.7.

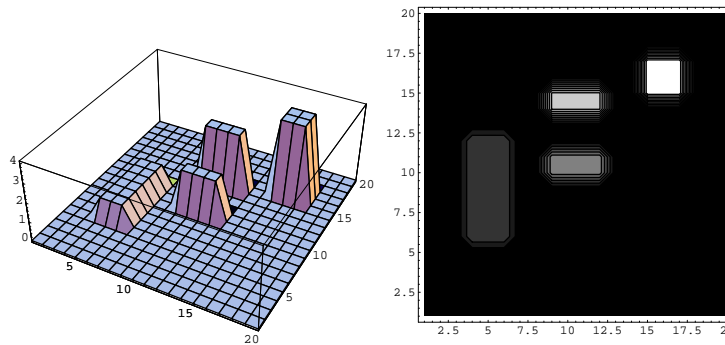


Fig. 7. The original function $f_2(x, y)$.

As was shown earlier (see, for example [4, 6, 7]), the image reconstruction of such objects from complete data gives a good enough results after 6-7 full iterations.

In this paper we present the numerical results of image reconstruction of chosen functions with two algebraic iterative algorithms ART-3 and MART-3 for two reconstruction schemes 1×1 and $(1 \times 1, 1 \times 1)$. We compare these results of reconstructions, and we investigate the influence of various parameters of these algorithms such as a pixel initialization, relaxation parameters, number of iterations and noise in the projection data on reconstruction quality. The convergence of these algorithms was studied in dependence on different these parameters. The convergence characteristic plots are given in view of plots for the maximum absolute error: $\Delta = \max_i |f_i - \bar{f}_i|$, the maximum relative error:

$$\delta\% = \frac{\max_i |f_i - \bar{f}_i|}{\max_i (f_i)} \cdot 100\%, \text{ and the mean absolute error } \delta = \frac{1}{n} \sum_i |f_i - \bar{f}_i|,$$

where f_i is the value of a given modeling function in the center of the i -th pixel and \bar{f}_i is the value of the reconstructed function in the i -th pixel.

The reconstruction result of $f_1(x, y)$ with algorithm ART-3 after 15 iterations in the reconstruction scheme $(1 \times 1, 1 \times 1)$ for $n = 20 \times 20$ pixels, $m = 644$ projections is presented in Fig.8. The plot of the reconstruction function is shown on the left side, and the plot of the mean absolute errors for this image reconstruction is shown on the right side.

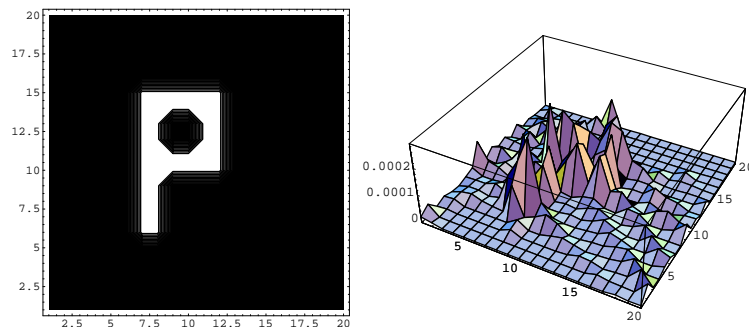


Fig. 8: The image reconstruction of $f_1(x, y)$ with ART-3 for $n = 20 \times 20$, $m = 644$, $iter = 15$ for the scheme $(1 \times 1, 1 \times 1)$.

For comparison this function $f_1(x, y)$ was reconstructed with multiplicative algorithm MART-3 for the same parameters and $\lambda = 6.9$ and the plots, which are presented in Fig. 9, illustrate the dependence of the maximum relative error and the mean absolute error on number of iterations with algorithms ART-3 and MART-3 in the system $(1 \times 1, 1 \times 1)$:

The same function $f_1(x, y)$ was also reconstructed in the system 1×1 . The result of this reconstruction with algorithm ART-3 for $n = 20 \times 20$, $m = 788$ and 100 iterations is shown in Fig. 10.

The plots, which are presented in Fig.11, illustrate the dependence of the maximum relative error and the mean absolute error on number of iterations of image reconstruction of $f_1(x, y)$ with algorithm ART-3 in the system $(1 \times 1, 1 \times 1)$ and in the system (1×1) :

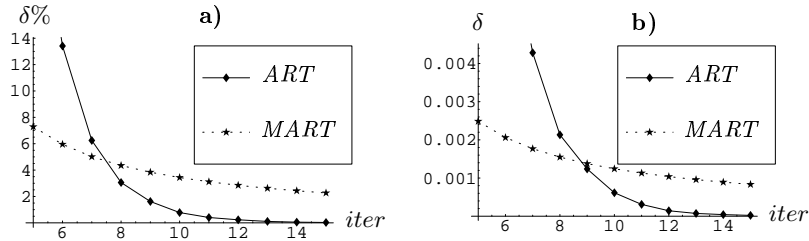


Fig. 9: Dependence of the maximum relative error (on the left side) and the mean absolute error (on the right side) on number of iterations for image reconstruction of $f_1(x, y)$ with algorithms ART-3 and MART-3 for $n = 400, m = 644$ in the system $(1 \times 1, 1 \times 1)$.

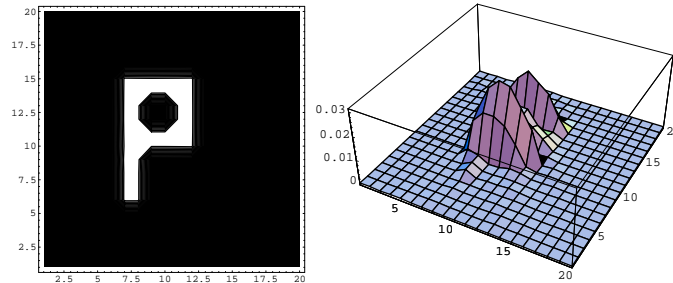


Fig. 10: The image reconstruction and the mean absolute error of $f_1(x, y)$ obtained with algorithm ART for $n = 20 \times 20, m = 788, iter = 100$ in the system 1×1 .

The analogous reconstructions were obtained for the function $f_2(x, y)$. The results of image reconstructions for $f_2(x, y)$ with algorithm ART-3 for the same parameters are given in Fig. 12.

The results of reconstruction of the function $f_2(x, y)$ in the system 1×1 is shown in Fig. 13

The plots presented in Fig.14 illustrate the dependence of the maximum relative error and the mean absolute error on the number of iterations of image reconstruction of $f_2(x, y)$ with algorithm ART-3 in the system $(1 \times 1, 1 \times 1)$ and in the system $(1 \times 1, 1 \times 1)$:

All experimental results in the case of reconstruction of objects from limited projection data showed that the errors of reconstruction is constantly reduced with increasing the number of iterations. The following table shows the dependence of the maximum absolute error on the number of iterations for the algorithm ART-3 for two systems (1×1) and $(1 \times 1, 1 \times 1)$ and the same set of parameters which were chosen above:

<i>iter</i>	100	200	500	1000	1297	2000	system
Δ	0.0306	0.00201	1.209×10^{-6}	6.435×10^{-12}	4.218×10^{-15}	5.44×10^{-15}	1×1
<i>iter</i>	10	20	40	50	60	105	system
Δ	0.0077	9.837×10^{-6}	3.127×10^{-11}	3.985×10^{-14}	6.661×10^{-16}	8.881×10^{-16}	$1 \times 1 \times 1$

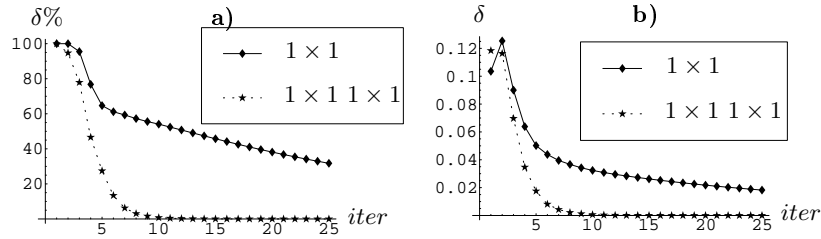


Fig. 11: Dependence of the maximum relative error (on the left side) and the mean absolute error (on the right side) of image reconstruction of $f_1(x, y)$ in the system $(1 \times 1, 1 \times 1)$ and in the system 1×1 .

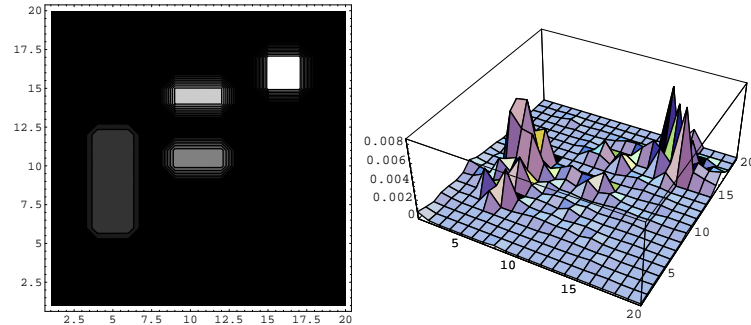


Fig. 12: The image reconstruction and the mean absolute error for $f_2(x, y)$ obtained with algorithm ART-3 for $n = 20 \times 20$, $m = 644$, $iter = 15$ in the system $(1 \times 1, 1 \times 1)$.

Note that the analogous table was obtained for algorithm MART-3, but in this case the velocity of convergence is considerably less.

For obtaining a good reconstruction in all experimental results it is very important, of course, the choice of the main parameters. From our investigation it follows that the best rate of convergence has the algorithm when the number of pixels (that is, the number of columns of an algebraic system of equations) is almost two times less than the number of all projection data (that is, the number of rows). The first parameter n , the number of pixels, was chosen in this paper in such a way that, in the first, the reconstructed function may be seen good enough on the picture, and, on the second, the obtained system of equations may be solved in the personal computer in a real time. The second main parameter m , the number of rays, was chosen in such a way that for some constant number of iteration $iter = 10$ (note, that for this number of iteration the quality of reconstruction was already obtained good enough) the reconstruction error was the least. For the system $(1 \times 1, 1 \times 1)$ the research for choosing m may be seen from the following table:

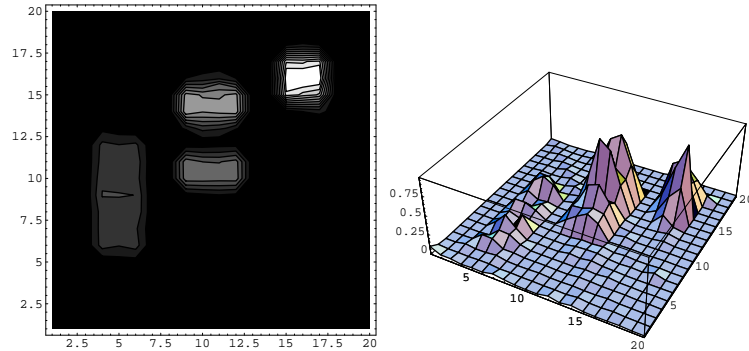


Fig. 13: The image reconstruction and the mean absolute error of $f_2(x, y)$ obtained with algorithm ART-3 for $n = 20 \times 20$, $m = 788$, $iter = 25$ in the system 1×1 .

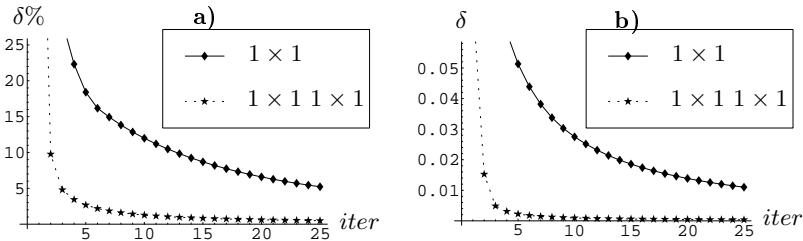


Fig. 14: Dependence of the maximum relative error (on the left side) and the mean absolute error (on the right side) of image reconstruction of $f_2(x, y)$ in the system $(1 \times 1, 1 \times 1)$ and in the system 1×1 .

$m = 28$	$m = 124$	$m = 288$	$m = 388$	$m = 644$	
1.000	0.544	0.073	0.0215	0.0077	Δ
100.0	54.42	7.328	2.1538	0.7793	$\delta\%$
0.122	0.029	0.002	0.0007	0.0006	δ

All algorithms were implemented on IBM/PC (procesor AMD Duron XP, 1600 MHz) by means of C++ and MATHEMATICA 5.1. One iteration by means of Mathematica 5.1 was implemented approximately 0.5s for algorithm ART-3 and 2.5s for algorithm MART-3, and in C++ one iteration for both algorithms is implemented in a real time.

5 Conclusion

The aim of this paper was an elaboration and comparison of the iterative algebraic algorithms for reconstruction of high-contrast objects from incomplete projection data. We study the quality and convergence of these algorithms. The experimental results show that for each considered scheme of reconstruction

there exist the parameters which allow to obtain an enough good quality of reconstruction after the number of iteration which is considerably larger than for reconstruction with complete projection data. The convergent characteristics of algorithm ART-3 are considerably better by comparison with algorithm MART-3. And the configuration $(1 \times 1, 1 \times 1)$ is considerably better by comparison with the scheme 1×1 . The number of iterations for achieving the stable reconstruction is approximately two times more for the second scheme by comparison with the first one. And this number is approximately 10 times more for the the scheme $(1 \times 1, 1 \times 1)$ by comparison with the case of the complete data. Moreover, if for the case of complete projection data there exists a number of iteration for which we have the best image reconstruction and after this number the error of reconstruction begins to increase, for the considered schemes of reconstruction with incomplete data the error of reconstruction reduces all time while it become stable and very small for enough large number (~ 1000).

References

1. Censor Y., De Piero A. R., Elfing T., Herman G. T., Iusem A. N.: *On iterative methods for linearly constrained entropy maximization*, In: Numerical Analysis and Math. Modeling, A.Wakulicz (ed.), v. 24, 145–163, Banach Center Publications, Warsaw, Poland, 1990.
2. Censor Y., Zenios S. A., *Parallel Optimization. Theory, Algorithms, and Applications*, Oxford University Press, 1997.
3. Eggermont P. P. B., Herman G. T., Lent A.: *Iterative algorithms for large partitioned linear systems with applications to image reconstruction*, Linear Algebra and Its Appl. v. **40** (1981), 37–67.
4. Gubareni N., *Computed Methods and Algorithms for Computer Tomography with limited number of projection data*, Naukova Dumka, Kiev, 1997. (in Russian).
5. Herman G. T.: *Image Reconstruction from Projections*, Academic Press, New York (1980).
6. Herman G. T.: *A relaxation method for reconstructing objects from noisy x-rays*, Math. Programming v. **8** (1975) 1–19.
7. Herman G. T., Lent A., Rowland S.: *ART: Mathematics and application (a report on the mathematical foundations and on the applicability to real data of the Algebraic Reconstruction Techniques)*, Journ. of Theoretica Biology v. **43** (1973), 1–32.
8. Lent A., *A convergent algorithm for maximum entropy image restoration, with a medical x-ray application*. In R.Shaw (ed), *Image Analysis and Evaluation*, 1977, p. 249–257. Society of Photographic Scientists and Engineers, Washington, USA.
9. Patella D.: *Introduction to ground surface self-potential tomography*, Geophysical Prospecting, vol. 45 (1997), 653–681.
10. Williams R. A., Atkinson K., Luke S. P., Barlow R. K., Dyer B. C., Smith J., Manning M.: *Applications for Tomographic Technology in Mining, Minerals and Food Engineering*, Particle and Particle Systems Characterization, vol. 12, N. 2 (2004) 105–111.